An Approach of Radar Reflectivity Data Assimilation and Its Assessment with the Inland QPF of Typhoon Rusa (2002) at Landfall

QINGNONG XIAO, YING-HWA KUO, JUANZHEN SUN, WEN-CHAU LEE, AND DALE M. BARKER

National Center for Atmospheric Research, Boulder, Colorado*

EUNHA LIM

Korea Meteorological Administration, Seoul, Korea

(Manuscript received 10 October 2005, in final form 20 April 2006)

ABSTRACT

A radar reflectivity data assimilation scheme was developed within the fifth-generation Pennsylvania State University–National Center for Atmospheric Research Mesoscale Model (MM5) three-dimensional variational data assimilation (3DVAR) system. The model total water mixing ratio was used as a control variable. A warm-rain process, its linear, and its adjoint were incorporated into the system to partition the moisture and hydrometeor increments. The observation operator for radar reflectivity was developed and incorporated into the 3DVAR. With a single reflectivity observation, the multivariate structures of the analysis increments that included cloud water and rainwater mixing ratio increments were examined. Using the onshore Doppler radar data from Jindo, South Korea, the capability of the radar reflectivity assimilation for the landfalling Typhoon Rusa (2002) was assessed. Verifications of inland quantitative precipitation forecasting (QPF) of Typhoon Rusa (2002) showed positive impacts of assimilating radar reflectivity data on the short-range QPF.

1. Introduction

Hurricane and typhoon forecasts have improved steadily over the past decade, primarily because of the increased use of remote sensing data over oceans to initialize tropical cyclones in numerical models (Harasti et al. 2004; Lee et al. 2004). There are, however, still several aspects that need scientific understanding and technical development for further improvement. For example, inland flooding is a chief cause of death and property damage associated with hurricane and typhoon landfall. Improving quantitative precipitation forecasting (QPF) related to hurricane/typhoon-induced flooding during landfall is a major objective of the U.S. Weather Research Program (Marks and Shay 1998; Elsberry 2002).

Doppler radar observations from onshore radar sites provide useful information about the storm structures of a tropical cyclone near landfall (Marks and Shay 1998; Marks 2003). How to incorporate such data optimally into the initialization of tropical cyclones for numerical prediction is a challenge. In recent years, the National Center for Atmospheric Research (NCAR) and the Korea Meteorological Administration (KMA) acted in partnership to develop Doppler radar data assimilation capability in the fifth-generation Pennsylvania State University–NCAR Mesoscale Model (MM5) three-dimensional variational data assimilation (3DVAR) system (Barker et al. 2003). The inclusion of the analyses (increments) of rainwater and cloud water mixing ratios in the 3DVAR system is vital to the development of radar reflectivity assimilation. The four-dimensional variational data assimilation (4DVAR) approach was usually used to retrieve all of these hydrometeor fields through reflectivity assimilation (Sun and Crook 1997, 1998). The ensemble Kalman filter technique has recently been tested to perform reflectivity assimilation in several studies (Dowell et al. 2004; Xue et al. 2006). In comparison with 4DVAR and ensemble Kalman filter techniques, the 3DVAR has its limita-

* The National Center for Atmospheric Research is sponsored by the National Science Foundation.

Corresponding author address: Qingnong Xiao, NCAR, MMM, P.O. Box 3000, Boulder, CO 80307-3000.
E-mail: hsiao@ucar.edu

DOI: 10.1175/JAM2439.1

tions in that the correlation or balance among the hydrometeors and other dynamical or thermodynamical variables is not easily defined under the 3DVAR framework. For example, it is not clear how the hydrometeors could induce increments in motion fields in 3DVAR. On the contrary, 4DVAR and ensemble Kalman filter methods that involve the whole model integration as a constraint are more effectively able to include these processes. In the continuous cycling mode, 3DVAR assimilation of radar reflectivity data can produce relatively rational analyses of the hydrometeor fields. A further significant advantage of 3DVAR is greater computational efficiency than 4DVAR or ensemble Kalman filter techniques.

This paper reflects a proof-of-concept study of the 3DVAR radar reflectivity assimilation using the landfalling Typhoon Rusa (2002) case. Radar observations of Typhoon Rusa (2002) from Jindo, an onshore radar site in South Korea, were supplemented into a cycled analysis of the MM5 3DVAR system at 3-hourly intervals for 1 day prior to landfall. Numerical forecasts were conducted with MM5 following the Doppler radar data assimilation to assess its impact on the prediction skills of a typhoon's inland precipitation.

2. Method

a. MM5 3DVAR

The configuration of the MM5 3DVAR system is based on a multivariate incremental formulation (Courtier et al. 1994). The preconditioned control variables in this study were streamfunction ψ, velocity potential χ, unbalanced pressure p_u, and total water mixing ratio q_t. Statistics of differences between 24-h forecasts and 12-h forecasts were used to estimate background error covariance; this method is the one proposed by Parrish and Derber (1992) for the National Meteorological Center (NMC) 3DVAR system (and hence it is called the NMC method). Horizontally isotropic and homogeneous recursive filters were applied to horizontal components of background error. The vertical component of background error was projected onto climatologically averaged [in time, longitude, and (optional) latitude] eigenvectors of vertical error estimated with the NMC method. A detailed description of the 3DVAR system can be found in Barker et al. (2003). The results of Doppler radial velocity assimilation for a frontal precipitation case are shown in Xiao et al. (2005).

b. Partitioning of moisture and hydrometeor increments

Radar reflectivity measures the radar's signal reflected by precipitation hydrometeors. To assimilate radar reflectivity directly, the MM5 3DVAR system should be able to produce the increments of the hydrometeors (at least the rainwater mixing ratio). However, the NMC method is not appropriate to perform the background error statistics for the rainwater mixing ratio, because it will result in zero errors in most of the domain grid points. Instead, we chose total water mixing ratio q_t as a control variable and conducted background error statistics for the MM5 3DVAR when radar reflectivity was to be assimilated. Because q_t was used as a control variable, partitioning of the moisture and hydrometeor increments was necessary in the 3DVAR system. In this study, we introduced the warm-rain process of Dudhia (1989), which includes condensation of water vapor into cloud (P_{CON}), accretion of cloud by rain (P_{RA}), automatic conversion of cloud to rain (P_{RC}), and evaporation of rain to water vapor (P_{RE}). These four are the major processes of the hydrometeor cycle in the summer season. For the Typhoon Rusa case, the collected Doppler radar data are mostly below 5 km and the warm-rain process should be a rational partitioning scheme for reflectivity assimilation.

The autoconversion term P_{RC} is represented by

$$P_{\mathrm{RC}} = \begin{cases} k_1(q_c - q_{\mathrm{crit}}), & q_c \geq q_{\mathrm{crit}} \\ 0, & q_c < q_{\mathrm{crit}} \end{cases}, \tag{1}$$

where q_c is the cloud water mixing ratio. According to Kessler (1969), $k_1 = 10^{-3}\ \mathrm{s}^{-1}$ and $q_{\mathrm{crit}} = 0.5\ \mathrm{g\ kg}^{-1}$. The accretion of cloud water by rain is parameterized by

$$P_{\mathrm{RA}} = \frac{1}{4}\pi\rho a q_c E N_0 \left(\frac{p_0}{p}\right)^{0.4} \frac{\Gamma(3+b)}{\lambda^{3+b}}, \tag{2}$$

where Γ is the gamma function, E is the collection efficiency, p is pressure, ρ is air density, λ is a coefficient defined in Dudhia (1989), $p_0 = 1000$ hPa, $N_0 = 8 \times 10^6\ \mathrm{m}^{-4}$, $a = 841.996\ 67$, and $b = 0.8$. The evaporation of rain can be determined from the equation

$$P_{\mathrm{RE}} = \frac{2\pi N_0 (S-1)}{A+B}\left[\frac{f_1}{\lambda^2} + f_2\left(\frac{a\rho}{\mu}\right)^{1/2} S_c^{1/3}\left(\frac{p_0}{p}\right)^{0.2} \frac{\Gamma\left(\frac{5+b}{2}\right)}{\lambda^{(5+b)/2}}\right], \tag{3}$$

where $f_1 = 0.78$ and $f_2 = 0.32$. The definitions of A, B, S, S_c, and μ are found in Dudhia (1989). The condensation $P_{\rm CON}$ is determined according to Asai (1965) by

$$P_{\rm CON} = \frac{q_v - q_{vs}}{1 + \dfrac{L_v^2 q_{vs}}{R_v C_{\rm pm} T^2}}, \tag{4}$$

where q_v is water vapor mixing ratio, q_{vs} is saturated water vapor mixing ratio, T is temperature, and L_v, R_v, and $C_{\rm pm}$ are latent heat of condensation, gas constant for water vapor, and specific heat at constant pressure for moist air, respectively.

The tangent linear and its adjoint of the scheme were developed and incorporated into the MM5 3DVAR system. Although the control variable is q_t, the q_v, q_c, and rainwater mixing ratio q_r increments are produced through the partitioning procedure during the 3DVAR minimization. The warm-rain parameterization builds a constraint: the relation among rainwater, cloud water, moisture, and temperature. When rainwater information (from reflectivity) enters the minimization iteration procedure, the forward warm-rain process and its backward adjoint distribute this information to the increments of other variables (under the constraint of the warm-rain scheme).

c. Observation operator for radar reflectivity

Once the 3DVAR system can produce q_c and q_r increments, the setup of the observation operator for assimilation of reflectivity is straightforward. In this study, we adopted the observation operator from Sun and Crook (1997):

$$Z = 43.1 + 17.5 \log(\rho q_r), \tag{5}$$

where Z is reflectivity (dBZ). The relation (5) is derived analytically by assuming the Marshall–Palmer distribution of raindrop size.

d. Some implementation details and procedure

Great efforts were made to incorporate the reflectivity assimilation into the MM5 3DVAR system. Figure 1 gives the flowchart of computations in the MM5 3DVAR minimization procedure. The new additions of the reflectivity assimilation components to the original 3DVAR minimization procedure are shaded. For clarity of the procedure, we summarized some implementation details in the following.

First of all, the control variable transform was built to bridge the control variables $\mathbf{v}$ and the analyzed variable increments $\mathbf{x}'$. The partitioning of the moisture and hydrometeor increments is added to the transform. Because we use q_t as a control variable, development of the linear warm-rain process is important to partition the q_v, q_c, and q_r increments. At the first iteration of the MM5 3DVAR minimization, the q_c and q_r increments are zero, and the q_v increment is equal to the q_t increment. We treated the warm-rain process as a column model. If any column is detected with updraft and supersaturation, an average of 30 min of updraft time is taken to produce the cloud water and rainwater using the one-dimensional column model. During the process, moisture and temperature should also be changed because of the condensation and evaporation involved in the process. When reflectivity observation is assimilated, the adjoint of the reflectivity operator will produce the cost function gradient with respect to the q_r by the adjoint of (5). The adjoint of moisture and hydrometeor partitioning scheme will distribute the information to the gradients with respect to q_c, q_v, and T and produce the gradient with respect to q_r. Afterward, the adjoint of the control variable transform will propagate the information to other variables and produce the cost function gradient of other control variables. The process is iterated back and forth in the MM5 3DVAR minimization procedure. When it converges, the increments of q_c, q_r, q_v, and T are produced by the reflectivity assimilation.

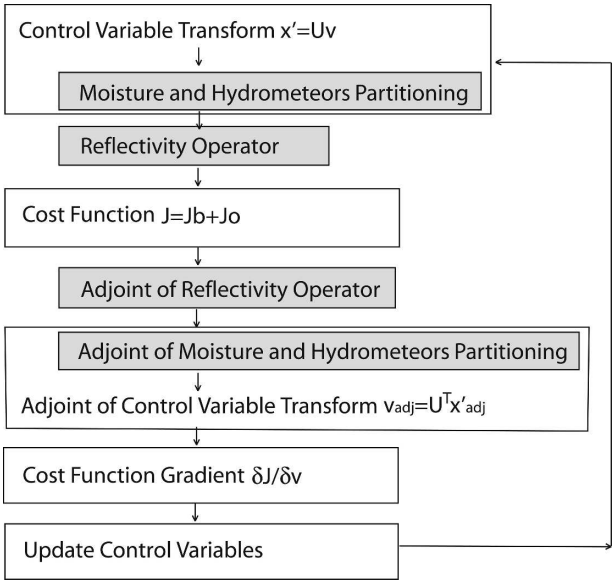

FIG. 1. Flowchart of the radar reflectivity data assimilation in minimization procedure of the MM5 3DVAR system. (The new additions of the reflectivity assimilation components to the 3DVAR are shaded.)

3. Typhoon Rusa (2002) at landfall and experimental design for its inland QPF

Typhoon Rusa was the most disastrous storm in Korea in 2002. It made landfall on the Korea south coast

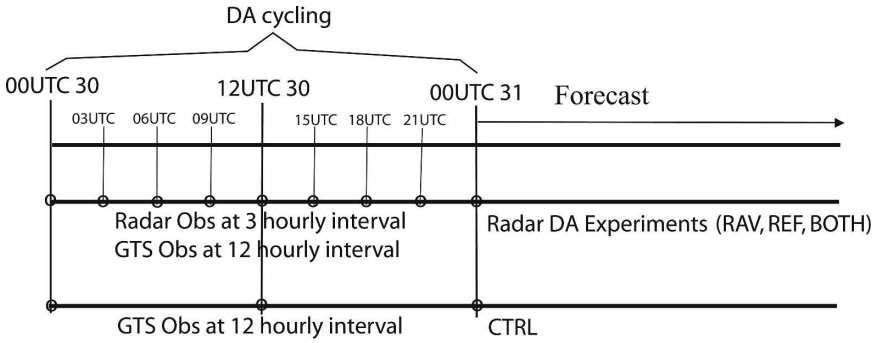

FIG. 2. Schematic diagram showing the frequency and types of observations assimilated with each experiment.

at 0630 UTC 31 August 2002 and dumped deadly torrential rainfall in a short time. Inland flooding was responsible for the death of more than 100 people in that nation. Prior to landfall, Rusa maintained the strength of central sea level pressure (CSLP) between 950 and 960 hPa for the whole of 30 August. After landfall it weakened rapidly, becoming an extratropical cyclone over the sea between the Republic of Korea and Japan on 1 September.

Jindo radar station is located on the southwestern tip of the Korean Peninsula. Prior to Rusa's (2002) landfall on the peninsula's south coast, Jindo radar started capturing the radial velocity and reflectivity data from 0000 UTC 30 August. We conducted 3DVAR data assimilation from 0000 UTC 30 through 0000 UTC 31 August with 3-hourly update cycling for 1 day. The initial time for numerical simulation is 0000 UTC 31 August 2002. In addition to conventional observations, the Jindo radar data at 3-hourly intervals were preprocessed and included in the 3DVAR cycled analyses. Doppler radar data preprocessing included quality control and mapping the data into gridded plan position indicator (PPI) coordinates before they were ingested into the 3DVAR analyses. We used the NCAR "SOLO" software (Oye et al. 1995) to edit the data manually and conduct quality control. The gridded PPI data were produced by NCAR's Sorted Position Radar Interpolation (SPRINT) and Custom Editing and Display of Reduced Information in Cartesian Space (CEDRIC) software, developed by Mohr and Vaughan (1979) and Mohr et al. (1981). The horizontal resolution of the processed data is 5 km. In the vertical direction there are nine elevations with the interval of 1°. All data in the mapping were from the same volume. The detailed processing procedure was described in Xiao et al. (2005). Numerical experiments were performed at a grid spacing of 10 km. Four experiments were made. A simple timeline chart with the frequency and types of observations assimilated with each experiment is shown in Fig. 2. In the "CTRL" experiment, conventional observations were assimilated at 12-h intervals during the cycling 3DVAR, followed by the MM5 forecast. The "RAV" experiment is the same as CTRL, but with Jindo radar radial velocity data assimilated from 0000 UTC 30 to 0000 UTC 31 August every 3 h. The technique of radial velocity data assimilation is described in Xiao et al. (2005). The "REF" experiment is the same as CTRL, but with Jindo radar reflectivity data assimilated from 0000 UTC 30 to 0000 UTC 31 August every 3 h. The "BOTH" experiment is the same as CTRL, but with both radial velocity and reflectivity data assimilated from 0000 UTC 30 to 0000 UTC 31 August every 3 h.

4. Test with a single reflectivity observation

The single observation test is an efficient way to determine how the observed information propagates to its vicinity via the established correlations among 3DVAR variables. In this section, we discuss the results of a single reflectivity observation test by conducting an experiment using the CTRL analysis at 0000 UTC 31 August as the first guess and assimilating the reflectivity at (34.314°N, 124.003°E; 3803.5 m) for the Jindo radar (asterisk in Figs. 3a and 5a, located at 34.471°N, 126.328°E; 499 m). This was a proof-of-concept test for understanding the response of the analysis increments to a single reflectivity observation. The innovation of this single reflectivity was assigned 2 dBZ. The background error covariance was from the statistics of the KMA operational forecasts in the summer month of July 2001 using the NMC method. Preconditioned control variables in the statistics were streamfunction, velocity potential, unbalanced pressure, and total water mixing ratio q_t; the hydrometeor partitioning process was applied in the 3DVAR physical transforms.

Figure 3 shows the 3DVAR analysis increment responses at 3803.5 m, the vertical height level converted from the elevation degree of the single reflectivity ob-

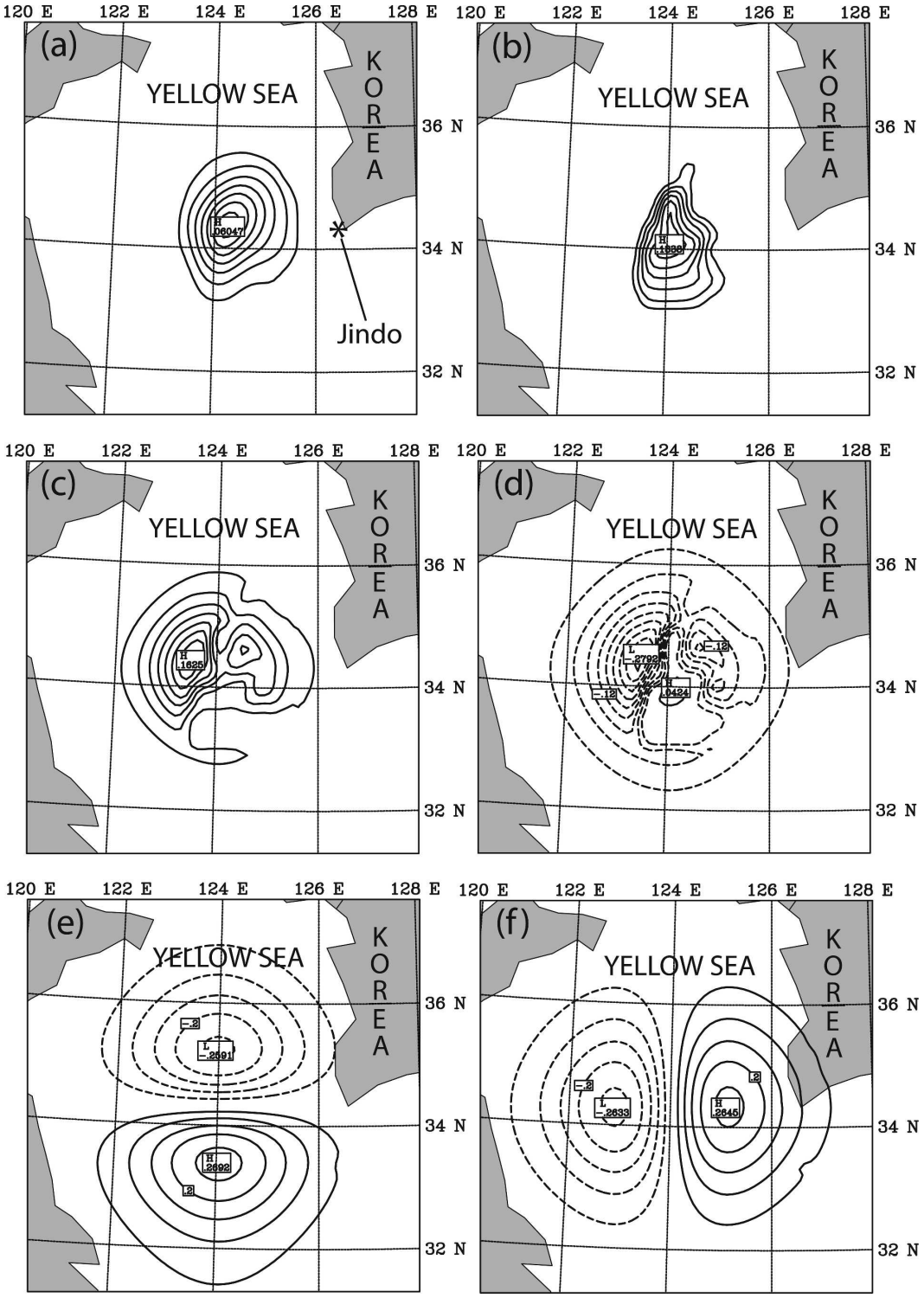

FIG. 3. Response of the analysis increments of (a) q_r (interval: 0.08 g kg^{-1}), (b) q_c (interval: 0.02 g kg^{-1}), (c) q_v (interval: 0.02 g kg^{-1}), (d) T (interval: 0.03 K), (e) wind component u (interval: 0.05 m s^{-1}), and (f) wind component v (interval: 0.05 m s^{-1}) to a single reflectivity observation with innovation of 2 dBZ at (34.314°N, 124.003°E; 3803.5 m) for the Jindo radar [asterisk in (a); located at 34.471°N, 126.328°E; 499 m].

servation. First of all, the rainwater mixing ratio q_r has positive analysis increments (Fig. 3a) in response to the assigned 2-dBZ innovation. Because the background error statistics using total water mixing ratio and hydrometeor partitioning (warm-rain process) were established in MM5 3DVAR, the analysis showed its multivariate nature. The cloud water mixing ratio q_c and the water vapor mixing ratio q_v presented positive analysis increments (Figs. 3b and 3c, respectively). The redistribution of hydrometeors in the water cycle also caused changes of temperature and winds. During the partitioning process, more evaporation (cooling) occurred from rainwater to water vapor than condensation (heating) from water vapor to cloud water; thus, the temperature increments presented a negative value (Fig. 3d). This is also the reason for the positive analysis increments of q_v. Figures 3e and 3f show the analysis increments of wind components u and v, respectively. Because of the MM5 3DVAR multivariate nature, the wind also showed cyclonic analysis increments in response to the 2-dBZ reflectivity innovation (through the forcing of temperature increments). The balance used in the 3DVAR increments could be used to explain why the cyclonic wind increments were produced with negative temperature increment (Fig. 3d). When an air column has temperature decreased (negative increments), it will reduce the depth of the air column and the isobaric surface will fall in the column. The geostrophic balance embedded in the 3DVAR increments will force the wind to produce cyclonic increments.

A distinct pattern in the hydrometeor analysis increments was its asymmetric distribution. Although an isotropic recursive filter was applied to the MM5 3DVAR background error covariance of the preconditioned control variables, the hydrometeor partitioning scheme caused the asymmetric incremental feature. The nonlinearity of the partitioning scheme described in section 2b is very strong. Its linearized scheme includes the background variables (i.e., background dependent). Because the background q_c and q_r were not continuous and their spatial variations were not homogeneous, the hydrometeor increments calculated by microphysics parameterization were not necessarily circularly symmetric. In Fig. 3, the maximum q_r increment (Fig. 3a) is in the single observation point, but the position of maximum q_c increment (Fig. 3b) shifts slightly southwestward. The center of other increments (temperature, water vapor, and wind components) also shifted (Figs. 3c–f). The shift of water vapor and temperature increments to the west might be caused by a gradient in the background humidity field with greater subsaturation to the west of the reflectivity observation location. The wind increments shift less westward than the temperature and water vapor increments, a compromise impact between the symmetric negative temperature increment centered on the reflectivity observation location and the westward-shifted asymmetric negative temperature increment shown in Fig. 3d. The background wind statistical correlation with unbalanced pressure might contribute to the pattern of the wind increments.

TABLE 1. The position error (km) and CSLP departure (hPa) of Typhoon Rusa (2002) in comparison with the best-track observation from the Tokyo Typhoon Center.

	Position error (km)			CSLP error (hPa)		
	0 h	6 h	12 h	0 h	6 h	12 h
CTRL	21.9	23.6	29.2	4.3	6.8	−7.0
RAV	11.8	10.9	29.1	4.1	6.1	−4.7
REF	17.1	11.3	29.1	4.2	6.3	−5.1
BOTH	11.8	18.3	25.5	4.2	4.9	−4.4

5. Inland QPF of Rusa (2002) at landfall

Typhoon Rusa made landfall at 0630 UTC 31 August 2002. At the forecast initial time (0000 UTC 31 August), the typhoon's outer rainband had started precipitating over the South Korea coast. Correct initialization of the typhoon at 0000 UTC 31 August was important for predicting imminent inland flooding. With the 1-day Doppler radar data continuously cycled into the MM5 3DVAR analyses, the initial typhoon vortex was relocated closer to the observed position in the radar data assimilation experiment (RAV, REF, or BOTH) than in CTRL. The initial typhoon CSLP intensities in RAV, REF, and BOTH also slightly improved relative to that of CTRL. Although slight, the largest improvement of the typhoon initial position and intensity was from the radial velocity assimilation experiment RAV. Table 1 shows that the typhoon position (CSLP) errors of CTRL, RAV, REF, and BOTH at 0000 UTC 31 August are 21.9 (4.3), 11.8 (4.1), 17.1 (4.2), and 11.8 (4.2) km (hPa), respectively. Subsequent 6- and 12-h forecast errors of the typhoon position and CSLP intensity (Table 1) were slightly reduced in RAV, REF, and BOTH experiments relative to those of CTRL. Improvements in the typhoon initialization and forecast in the Doppler radar data assimilation experiments enhanced the subsequent QPF skill. Figure 4 presents the 3-h rainfall verification of the equitable threat score (ETS; Rogers et al. 1996) for 12 h; results clearly indicate that assimilation of Doppler radar data had a positive impact on a short-range rainfall forecast. Rainfall verification was performed using Korean high-resolution Automatic

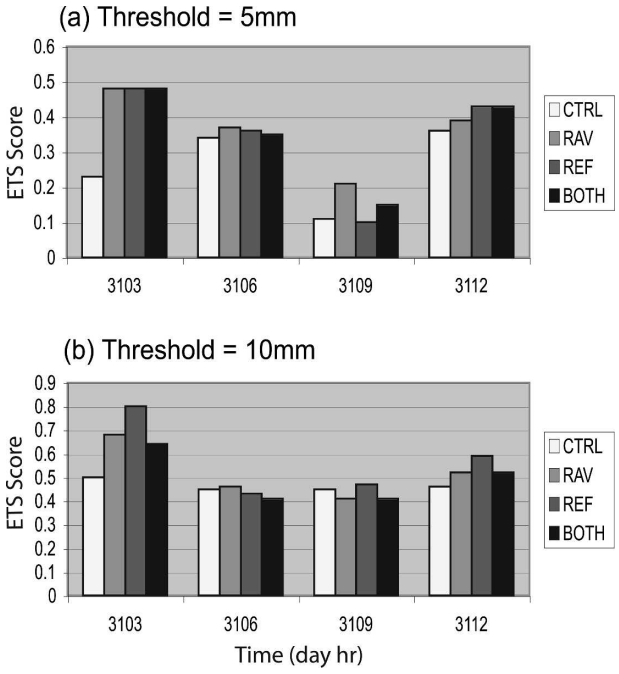

FIG. 4. Equitable threat scores of 3-h rainfall simulations for experiments CTRL, RAV, REF, and BOTH with threshold = (a) 5 and (b) 10 mm.

Weather Station hourly rainfall observations. In general, the average ETS of the RAV, REF, or BOTH experiment was higher than that of the experiment without radar data assimilation (CTRL). The positive impact of radar reflectivity assimilation (REF) appeared mainly in the first 3-h forecast. The positive impact of radial velocity assimilation (RAV), however, existed in the 6-h forecast. The results in the 9-h rainfall verification were mixed. The decrease of ETS scores in REF after 3 h and then the increase again after 9 h indicated that the rainfall forecast underwent an adjusting process in the REF experiment. Even though REF matched the rainfall very well in the beginning, there were imbalances in the analyses resulting from the difference of the warm-rain process in 3DVAR and the microphysics in the model. At the 12-h forecast, the ETS scores were higher in the RAV, REF, and BOTH experiments than in CTRL. For heavy rainfall (threshold of 10 mm), the reflectivity assimilation experiment (REF) obtained the highest ETS score among the four experiments at the 12-h forecast. Doppler radar data assimilation experiments produced noticeable positive impacts that lasted for 12 h.

The experiment REF in Fig. 4 presented a notably high ETS score at 0300 UTC 31 August. To display the rainfall structure more clearly at this time, Fig. 5 shows the composite reflectivity for the observation (Fig. 5a) as well as the forecasts by CTRL (Fig. 5b) and REF

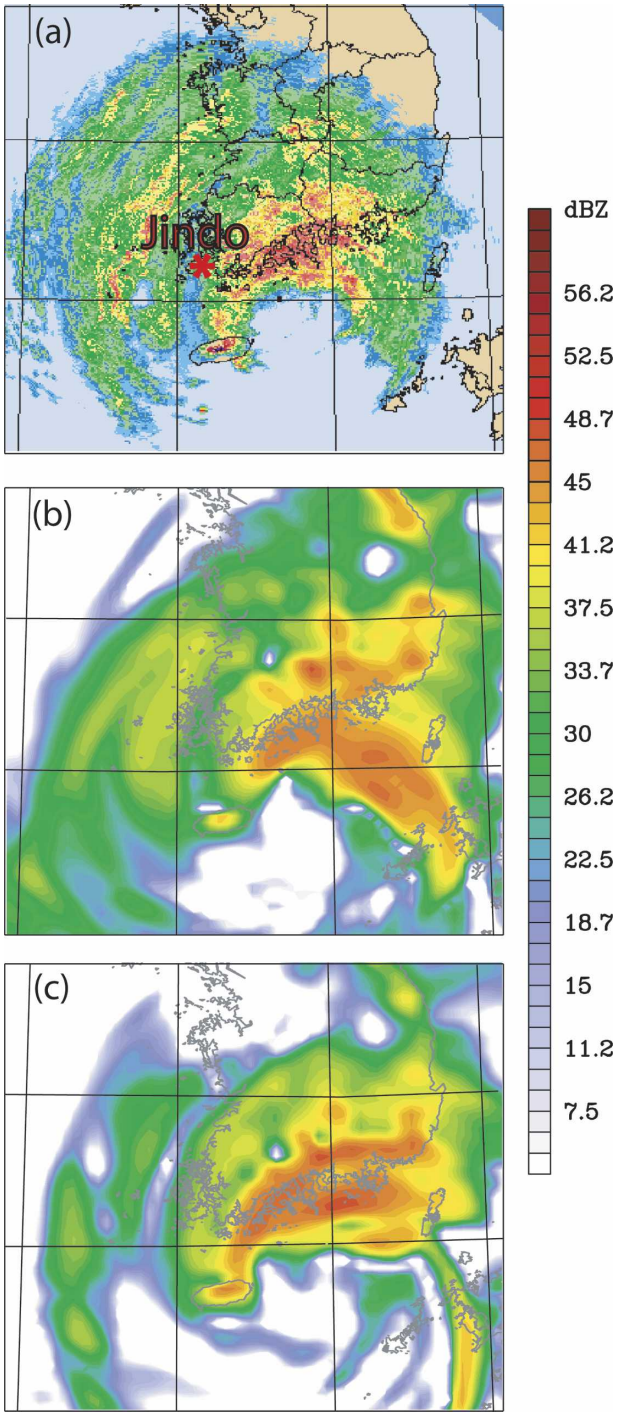

FIG. 5. Radar reflectivity at 0300 UTC 31 Aug 2002 for (a) observation, (b) experiment CTRL, and (c) experiment REF. The color bar on the right side of the figure shows the scales of the reflectivity. Jindo radar station is shown with an asterisk in (a).

(Fig. 5c) at 0300 UTC 31 August (3-h forecast). Here composite reflectivity is defined as the maximum reflectivity in the vertical column (Xue and Martin 2006); and the model reflectivity is derived from the predicted

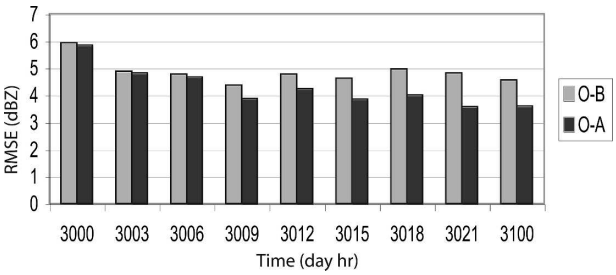

FIG. 6. Reflectivity RMSE before (O-B) and after (O-A) 3DVAR procedure during the 1-day Doppler reflectivity data cycling from 0000 UTC 30 to 0000 UTC 31 Aug 2002.

hydrometeors, including rainwater, snow, and hail mixing ratios using the MM5 output diagnosis Read/Interpolate/Plot (RIP) software. The rainfall distribution in Fig. 5c is much closer to the observation (Fig. 5a) than the distribution of the experiment without radar data assimilation (Fig. 5b).

Doppler reflectivity data mostly contain precipitation hydrometeor information. Assimilation of Doppler reflectivity data is usually difficult with a 3DVAR approach in which hydrometeor variables are not included. In the new development of this study, total water content was used as a control variable and a warm-rain partitioning scheme was incorporated into the 3DVAR physical transforms. The radar reflectivity information could be ingested into the 3DVAR analysis, and positive impacts on the short-range QPF skill were observed. To show the effectiveness of Doppler reflectivity assimilation in the MM5 3DVAR cycling run, Fig. 6 depicts how the analyzed reflectivity fits to observations during the 3DVAR cycling procedure from 0000 UTC 30 through 0000 UTC 31 August. In each cycle, the root-mean-square error (RMSE) of the analysis (O-A) was smaller than the RMSE of the background reflectivity (O-B). For most of the two consecutive cycles, the RMSE of the 3DVAR analysis in the later cycle was smaller than in its previous cycle. There was a general decrease of the analyzed reflectivity RMSE with the increase of the cycling from 0000 UTC 30 to 0000 UTC 31 August. This showed that the 3DVAR cycling procedure works well. Assimilation of Doppler reflectivity with a cycling mode gradually extracts useful information from Doppler reflectivity data and improves the forecast skill.

6. Discussion and conclusions

The MM5 3DVAR system with the capability of assimilating Doppler reflectivity data has been developed. Note that the method by which observed reflectivity information propagates to other fields is very different in the MM5 3DVAR versus the 4DVAR. MM5 4DVAR uses the model with full physics to constrain the propagation, whereas MM5 3DVAR uses the background error correlations and balance constraint (including the partitioning scheme). Because 3DVAR is very computationally efficient, we can conduct rapid update cycling to extract the model dynamic constraint into the analysis. How the effectiveness of the 3DVAR rapid update cycling versus the 4DVAR varies is now under research.

Meanwhile, the capability of the developed Doppler radar data assimilation scheme in the MM5 3DVAR was thoroughly tested in KMA. The length scales were statistically tuned based on the method of Desroziers and Ivanov (2001). Parallel runs, with and without radar data, were executed to assess the impact of the Doppler radar data assimilation in KMA preoperational testing. The results were positive. Doppler radar data assimilation improved the short-range QPF skills when compared with the forecasts without radar data assimilation; the QPF scores are improved up to the 12-h forecast (E. Lim 2005, unpublished work). The developed radar data assimilation is currently in operation during the summer season in KMA.

In the research in this paper, it is found that the new 3DVAR radar reflectivity assimilation approach has a multivariate feature among the dynamic, thermodynamic, and hydrometeor variables in the analyses. The inclusion of hydrometeor increments in the MM5 3DVAR multivariate correlation structure is important for radar reflectivity assimilation. We obtained the following conclusions based on its assessment of the short-range QPF skills for the landfalling Typhoon Rusa (2002) case:

1) The MM5 3DVAR system with a 3-h cycling interval of the observed Doppler reflectivity data efficiently incorporates useful information into a typhoon's initial conditions. The observed reflectivity information can propagate to the hydrometeor, thermodynamic, and dynamic fields of the typhoon analysis.
2) Assimilation of Doppler reflectivity data improves the inland short-range QPF skill. The positive impact appeared mainly in the first 3-h forecast. A noticeable positive impact on the rainfall forecast was observed for up to 12 h when both radial velocity and reflectivity data from onshore Doppler radar were assimilated into the typhoon's initial conditions.
3) Typhoon Rusa was adjusted toward the observed position during the 3DVAR cycling of the Doppler

radar data. Because the typhoon initialization was improved by Doppler radar data assimilation, its subsequent typhoon forecast and its QPF were also improved.

The method of the Doppler radar data assimilation in MM5 3DVAR is now transferred to the Weather Research and Forecasting (WRF) 3DVAR system. We are working toward evaluation of the scheme in the Advanced Research WRF (ARW), which is a new mesoscale model. Addition of the ice phase in the hydrometeor partitioning scheme is planned to facilitate its more broad applications (especially in the winter season). One simple way to achieve this addition is based on the MM5 simple ice scheme such that the same warm-rain process is used for the ice-phase process when the background temperature is below the freezing point. How this simple ice scheme works in the 3DVAR system requires further research. There are great challenges in this important area in the future.

Acknowledgments. The authors are very grateful to Andrew C. Lorenc of the Met Office for motivating us to implement a hydrometeor partitioning scheme in MM5 3DVAR during his visit to NCAR in 2003. Discussions with Jimy Dudhia of NCAR/MMM about the warm-rain process were very helpful for the incorporation of the scheme into the MM5 3DVAR system. This research is supported by the USWRP project and Korea Meteorological Administration.

REFERENCES

Asai, T., 1965: A numerical study of the air-mass transformation over the Japan Sea in winter. *J. Meteor. Soc. Japan,* **43,** 1–15.

Barker, D. M., W. Huang, Y.-R. Guo, and A. Bourgeois, 2003: A three-dimensional variational (3DVAR) data assimilation system for use with MM5. NCAR Tech. Note NCAR/TN-453+STR, 68 pp.

Courtier, P., J. N. Thepaut, and A. Hollingsworth, 1994: A strategy for operational implementation of 4D-Var using an incremental approach. *Quart. J. Roy. Meteor. Soc.,* **120,** 1367–1387.

Desroziers, G., and S. Ivanov, 2001: Diagnosis and adaptive tuning of observation-error parameters in a variational assimilation. *Quart. J. Roy. Meteor. Soc.,* **127,** 1433–1452.

Dowell, C. D., F. Zhang, L. J. Wicker, C. Snyder, and N. A. Crook, 2004: Wind and temperature retrievals in the 17 May 1981 Arcadia, Oklahoma, supercell: Ensemble Kalman filter experiments. *Mon. Wea. Rev.,* **132,** 1982–2005.

Dudhia, J., 1989: Numerical study of convection observed during the winter monsoon experiment using a mesoscale two-dimensional model. *J. Atmos. Sci.,* **46,** 3077–3107.

Elsberry, R. L., 2002: Predicting hurricane landfall precipitation: Optimistic and pessimistic views from the symposium on precipitation extremes. *Bull. Amer. Meteor. Soc.,* **83,** 1333–1340.

Harasti, P. R., C. J. McAdie, P. P. Dodge, W.-C. Lee, J. Tuttle, S. T. Murillo, and F. D. Marks Jr., 2004: Real-time implementation of single-Doppler radar analysis methods for tropical cyclones: Algorithm improvements and use with WSR-88D display data. *Wea. Forecasting,* **19,** 219–239.

Kessler, E., 1969: *On the Distribution and Continuity of Water Substance in Atmospheric Circulation. Meteor. Monogr.,* No. 32, Amer. Meteor. Soc., 84 pp.

Lee, J.-L., A. E. MacDonald, Y.-H. Kuo, W.-C. Lee, and W. Wang, 2004: Use of radar data for TC initialization and predictions. *Proc. 26th Conf. on Hurricanes and Tropical Meteorology,* Miami, FL, Amer. Meteor. Soc., 554–557.

Marks, F., 2003: State of the science: Radar view of tropical cyclone. *Radar and Atmospheric Science: A Collection of Essays in Honor of David Atlas, Meteor. Monogr.,* No. 52, Amer. Meteor. Soc., 33–75.

——, and L. K. Shay, 1998: Landfalling tropical cyclones: Forecast problems and associated research opportunities. *Bull. Amer. Meteor. Soc.,* **79,** 305–323.

Mohr, C. G., and R. L. Vaughan, 1979: An economical procedure for Cartesian interpolation and display of radar data to three-dimensional space. *J. Appl. Meteor.,* **18,** 661–670.

——, L. J. Miller, and R. L. Vaughan, 1981: An interactive software package for the rectification of radar data to three-dimensional Cartesian coordinates. Preprints, *20th Conf. on Radar Meteorology,* Boston, MA, Amer. Meteor. Soc., 690–695.

Oye, R., C. Mueller, and S. Smith, 1995: Software for radar translation, visualization, editing, and interpolation. Preprints, *27th Conf. on Radar Meteorology,* Vail, CO, Amer. Meteor. Soc., 359–361.

Parrish, D. F., and J. C. Derber, 1992: The National Meteorological Center's spectral statistical interpolation analysis system. *Mon. Wea. Rev.,* **120,** 1747–1763.

Rogers, E., T. L. Black, D. G. Deaven, and G. J. DiMego, 1996: Changes to the operational "early" Eta analysis/forecast system at the National Centers for Environmental Prediction. *Wea. Forecasting,* **11,** 391–413.

Sun, J., and N. A. Crook, 1997: Dynamical and microphysical retrieval from Doppler radar observations using a cloud model and its adjoint. Part I: Model development and simulated data experiments. *J. Atmos. Sci.,* **54,** 1642–1661.

——, and ——, 1998: Dynamical and microphysical retrieval from Doppler radar observations using a cloud model and its adjoint. Part II: Retrieval experiments of an observed Florida convective storm. *J. Atmos. Sci.,* **55,** 835–852.

Xiao, Q., Y.-H. Kuo, J. Sun, W.-C. Lee, E. Lim, Y.-R. Guo, and D. M. Barker, 2005: Assimilation of Doppler radar observations with a regional 3DVAR system: Impact of Doppler velocities on forecasts of a heavy rainfall case. *J. Appl. Meteor.,* **44,** 768–788.

Xue, M., and W. Martin, 2006: A high-resolution modeling study of the 24 May 2002 dryline case during IHOP. Part I: Numerical simulation and general evolution of the dryline and convection. *Mon. Wea. Rev.,* **134,** 149–171.

——, M. Tong, and K. K. Droegemeier, 2006: An OSSE framework based on the ensemble square root Kalman filter for evaluating the impact of data from radar networks on thunderstorm analysis and forecasting. *J. Atmos. Oceanic Technol.,* **23,** 46–66.